GEOLOGY

The tempo of Ediacaran evolution

Chuan Yang[1]*, Alan D. Rooney[2]*, Daniel J. Condon[1], Xian-Hua Li[3,4], Dmitriy V. Grazhdankin[5,6], Fred T. Bowyer[7]†, Chunlin Hu[4,8], Francis A. Macdonald[9], Maoyan Zhu[4,8]*

The rise of complex macroscopic life occurred during the Ediacaran Period, an interval that witnessed large-scale disturbances to biogeochemical systems. The current Ediacaran chronostratigraphic framework is of insufficient resolution to provide robust global correlation schemes or test hypotheses for the role of biogeochemical cycling in the evolution of complex life. Here, we present new radio-isotopic dates from Ediacaran strata that directly constrain key fossil assemblages and large-magnitude carbon cycle perturbations. These new dates and integrated global correlations demonstrate that late Ediacaran strata of South China are time transgressive and that the 575- to 550-Ma interval is marked by two large negative carbon isotope excursions: the Shuram and a younger one that ended ca. 550 Ma ago. These data calibrate the tempo of Ediacaran evolution characterized by intervals of tens of millions of years of increasing ecosystem complexity, interrupted by biological turnovers that coincide with large perturbations to the carbon cycle.

INTRODUCTION

The Ediacaran Period [635 to 539 million years (Ma) ago] is a pivotal period in Earth history, archiving the rise of complex macroscopic life (*1*). This evolutionary milestone occurred in the aftermath of extreme climate perturbations, the Cryogenian snowball Earth events (*2*), and amid several perturbations to the carbon cycle. These are recorded by large carbon-isotope excursions (CIEs) in marine carbonate records, defined as negative and positive deviations in the stratigraphic trend of carbonate-carbon isotope ($\delta^{13}C_{carb}$) profiles. These perturbations have been documented worldwide and are commonly used to establish regional to global stratigraphic correlations (*1*, *3*, *4*).

Integration of Ediacaran datasets from geographically disparate localities has relied upon bio-, litho-, and chemostratigraphic correlation combined with sparse radio-isotopic ages. Within this framework, the Ediacaran has been divided into a lower series characterized by abundant and taxonomically diverse acanthomorphic acritarch assemblages and an upper series with Ediacara-type macrofossils (*1*). The ca. 580-Ma Gaskiers glaciation is commonly depicted to mark the boundary between the two series; however, because the Gaskiers glaciation in Newfoundland is interpreted as a regional glaciation, its relevance for global correlation remains unclear (*5*). Furthermore, direct age constraints on early Ediacaran acritarch assemblages and late Ediacaran macrofossil assemblages, and their age ranges, are generally lacking, precluding a more refined subdivision of Ediacaran time and early animal evolution. Consequently, it remains debated if the stratigraphic expression of the Ediacaran fossil record through the lens of preservation is a consequence of evolutionary and/or environmental drivers (*6*, *7*).

The Shuram CIE, the largest magnitude negative excursion in Earth history with $\delta^{13}C_{carb}$ values as low as −12‰ and sustained over considerable stratigraphic thickness, has been a major focus for Ediacaran chronostratigraphic correlation (*3*, *8*, *9*). Occurrence of such a distinct CIE in most of the regions within upper Ediacaran stratigraphy has been used to drive and support global correlation of these sections (*1*, *10*). Previous age models, assuming a single CIE, have estimated its onset to between 580 and 560 Ma ago with termination by ca. 551 Ma ago, as marked by a chemical abrasion–isotope dilution–thermal ionization mass spectrometry (CA-ID-TIMS) zircon U-Pb date from the uppermost Doushantuo Formation (Fm) of South China (*8*, *11*). However, the correlation between this U-Pb date and the Shuram has aroused heated debate, sparked by the regional stratigraphic complexity of the Doushantuo and Dengying Fms in South China (*12*, *13*). Recent Re-Os geochronological data from northwestern (NW) Canada and Oman instead suggest that the Shuram is shorter in duration (<10 Ma) and terminated >15 Ma earlier than previously thought (*4*), bringing into question whether a single negative CIE characterizes this time interval. Meanwhile, considerable debate remains regarding the extent to which these Ediacaran CIEs can be used to reconstruct the global carbon cycle and redox budgets, as well as their utility for correlation (*14*, *15*). Mechanistic and correlation uncertainties are fueled by the lack of a chronostratigraphic framework at sufficient resolution for testing hypotheses related to the tempo, magnitude/duration of the events, their global expression, or their co-relationship with biospheric evolutionary innovations.

Ediacaran stratigraphic successions developed in various facies ranging from shallow to deep marine settings in South China host extraordinarily well-preserved fossil assemblages. These assemblages include the acanthomorphic acritarchs; the Lantian, Weng'an, Wenghui, and Miaohe biotas of the Doushantuo Fm; and a morphologically complex, mixed assemblage of Ediacaran-type body fossils, tubular forms, and trace fossils of the Dengying Fm (*16*). These fossil records provide insights into taphonomic variations, body plan evolution, the paleogeographic distribution of macroscopic organisms, and the influence of oscillating redox conditions at the dawn of animal life (*17*–*19*). Here, we present new U-Pb zircon and

[1]Geochronology and Tracers Facility, British Geological Survey, Keyworth NG12 5GG, UK. [2]Department of Earth and Planetary Sciences, Yale University, New Haven, CT 06511, USA. [3]State Key Laboratory of Lithospheric Evolution, Institute of Geology and Geophysics, Chinese Academy of Sciences, Beijing 100029, China. [4]College of Earth and Planetary Sciences, University of Chinese Academy of Sciences, Beijing 100049, China. [5]Precambrian Palaeontology and Stratigraphy Laboratory, Trofimuk Institute of Petroleum Geology and Geophysics, prospect Akademika Koptyuga 3, Novosibirsk 630090, Russia. [6]Novosibirsk State University, ulitsa Pirogova 1, Novosibirsk 630090, Russia. [7]School of Earth and Environment, University of Leeds, Leeds LS2 9JT, UK. [8]State Key Laboratory of Palaeobiology and Stratigraphy & Center for Excellence in Life and Paleoenvironment, Nanjing Institute of Geology and Palaeontology, Chinese Academy of Sciences, Nanjing 210008, China. [9]Department of Earth Science, University of California Santa Barbara, Santa Barbara, CA 93106, USA. *Corresponding author. Email: chuany@bgs.ac.uk (C.Y.); alan.rooney@yale.edu (A.D.R.); myzhu@nigpas.ac.cn (M.Z.)
†Present address: School of GeoSciences, University of Edinburgh, James Hutton Road, Edinburgh EH9 3FE, UK.

Re-Os black shale radio-isotope geochronology and $\delta^{13}C_{carb}$ data from key Ediacaran successions of South China (Fig. 1). Updated U-Pb zircon dates from fossiliferous late Ediacaran strata of the White Sea area, East European Platform are also included. These new data are then integrated with existing global radio-isotopic geochronology and carbon isotope chemostratigraphic data. We review, reconsider stratigraphic contexts of the Ediacaran fossil record, uncertainties arising from stratigraphy and geochronology, and reassess the pattern and dynamics of Ediacaran CIEs to address the regional stratigraphic complexity (e.g., South China) and present a refined temporal framework for the rise and early evolution of complex macroscopic life.

RESULTS

New Ediacaran radio-isotopic dates along with their stratigraphic context are given in table S1 and outlined below. These include six zircon U-Pb dates and two black shale Re-Os dates from South China and two zircon U-Pb dates from the White Sea area of the East European Platform. Plots of U-Pb and Re-Os data are presented in fig. S1. Details of the studied locations in South China and of our CA-ID-TIMS zircon U-Pb, black shale Re-Os, and C-isotope data are given in the Supplementary Materials (figs. S2 to S4 and tables S2 to S4). A complete list of radio-isotopic dates that constrain Ediacaran stratigraphy is presented in table S5. Unless otherwise stated, errors of radio-isotopic dates are presented in 2-sigma as total uncertainty (analytical + calibration).

South China

During the Ediacaran Period, a shallow marine platform, slope, and deep basin formed across the southeast margin of the Yangtze Block of South China. Through this succession, several CIEs have been identified and associated with various fossil assemblages (Fig. 1 and fig. S2) (*11*, *20*, *21*). The Doushantuo Fm (ca. 635 to 551 Ma ago) ranges in thickness from <40 to >100 m and is composed predominantly of black shale and carbonate. Large lateral facies change is associated with different depositional environments from platform to basin. Several decades of work has led to the development of a $\delta^{13}C_{carb}$ framework for the Doushantuo Fm that has identified several negative CIEs including a large-magnitude excursion in the upper Doushantuo (Fig. 1) that has been correlated with the dated Shuram CIE of Oman and NW Canada (Fig. 2).

In western Hubei Province platform settings, the zircon U-Pb date of 609 ± 5 Ma (*22*) from the base of Unit 5 of the Doushantuo Fm at Zhangcunping section was interpreted as an age constraint on the Weng'an biota. Our new CA-ID-TIMS U-Pb analyses of zircons from this sample indicate their detrital origin, and the youngest CA-ID-TIMS date of 612.5 ± 0.9 Ma provides the maximum depositional age (Fig. 1). A new Re-Os date of 587.2 ± 3.6 Ma from a horizon 58 m above the base of Doushantuo Fm at the Jiulongwan section provides a maximum age constraint on the onset of the Shuram CIE (Fig. 1). In addition, this Re-Os date could be correlated using chemostratigraphy and sequence stratigraphy to the boundary between the *Tanarium tuberosum–Schizofusa zangwenlongii* and *Tanarium conoideum–Cavaspina basiconica* microfossil assemblage zones (*17*) and the lowest part of Weng'an biota (*11*). We note that this correlation remains controversial (*11*, *23*); further discussions of these correlations and the age of Weng'an biota are given in the Supplementary Materials. An ash bed from the top of the Miaohe Member of the Doushantuo Fm at the Jijiawan section in the western

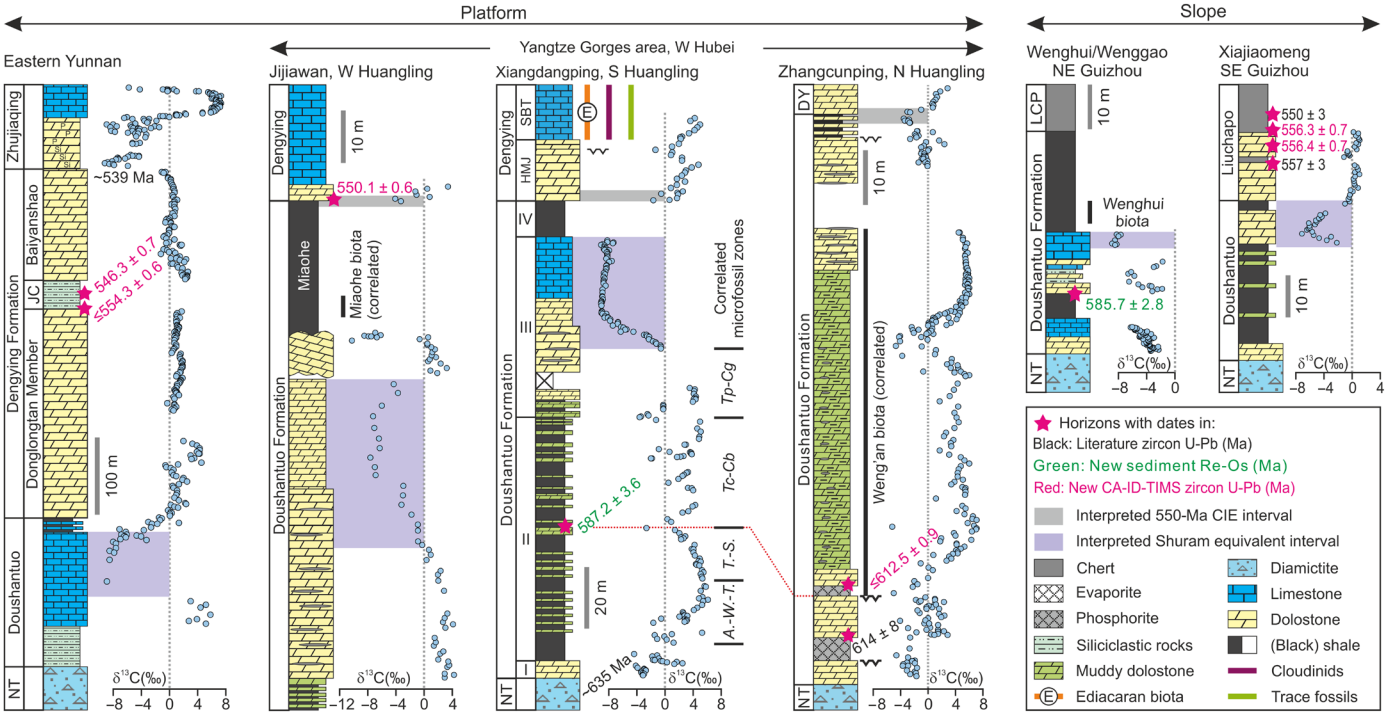

Fig. 1. Neoproterozoic-Cambrian stratigraphy, South China. Stratigraphic data sources: Eastern Yunnan (*21*, *54*), Jijiawan (*3*), Xiangdangping (*11*, *12*, *17*), Zhangcunping (*23*, *55*), Wenghui (*56*), and Xiajiaomeng (this study). Ages in black are from (*8*, *28*, *57*). DY, Dengying Fm; LCP, Liuchapo Fm; JC, Jiucheng Member; HMJ, Hamajing Member; SBT, Shibantan Member; NT, Nantuo Fm; *A.-W.-T.*, *Appendisphaera grandis–Weissiella grandistella–Tianzhushania spinose*; *T.-S.*, *Tanarium tuberosum–Schizofusa zangwenlongii*; *Tc-Cb*, *Tanarium conoideum–Cavaspina basiconica*; *Tp-Cg*, *Tanarium pycnacanthum–Ceratosphaeridium glaberosum*.

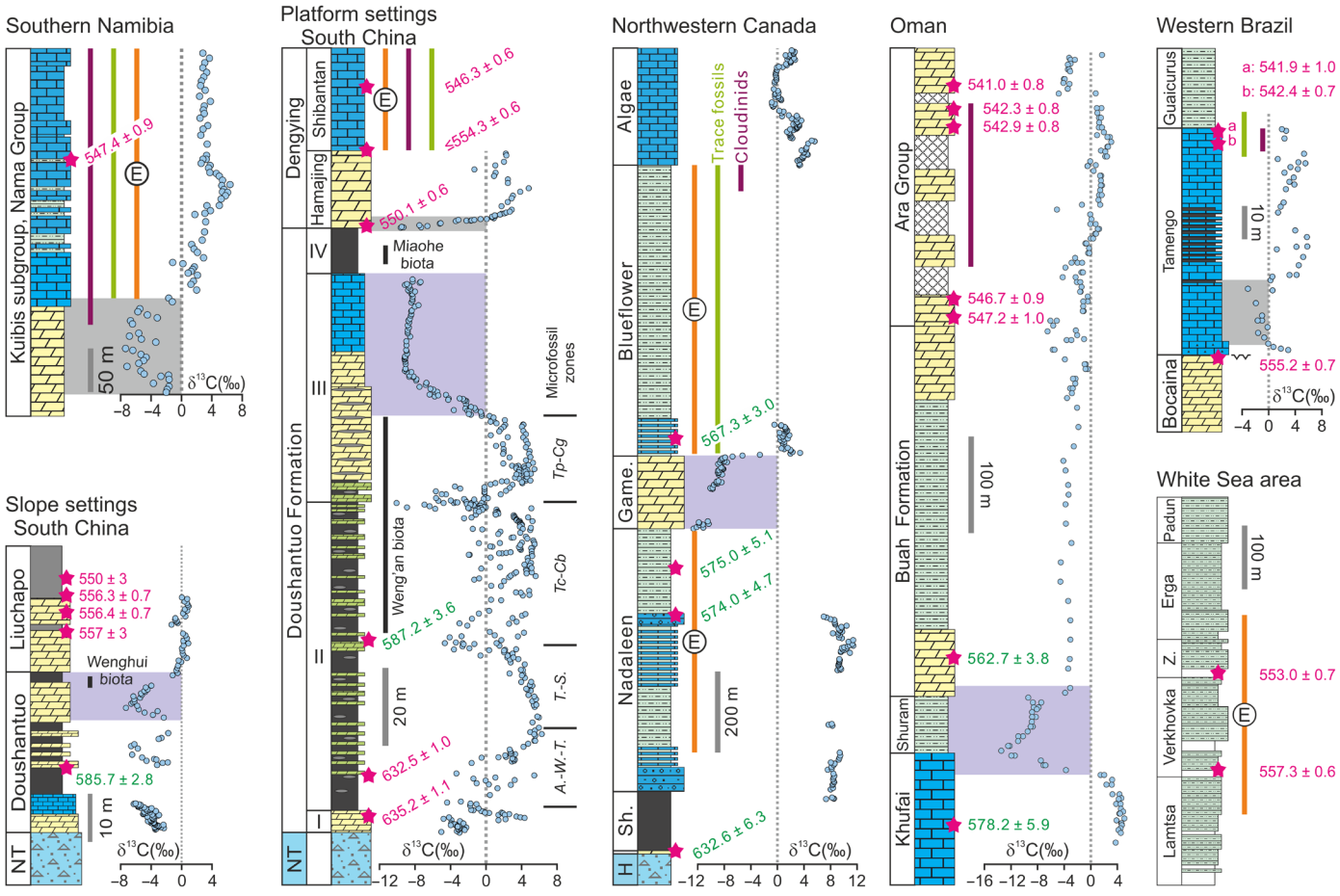

Fig. 2. Composite sections of Neoproterozoic-Cambrian transitional stratigraphy. Stratigraphic data sources: southern Namibia (*10*, *58*), South China–Slope (this study), South China–Platform (table S6), northwestern Canada (*4*, *43*), Oman (*4*, *10*), western Brazil (*32*, *59*), and White Sea area (this study). Zircon U-Pb and sediment Re-Os dates are in red and purple, respectively. For other symbols, see legend on Fig. 1.

region of Huangling Anticline, where the $\delta^{13}C_{carb}$ values increase from −3.2‰ to +3.6‰, has a revised age of 550.1 ± 0.6 Ma (Fig. 1). Uncertainty exists in the stratigraphic position of this age relative to the Shuram excursion because of controversy regarding the upper boundary of this CIE in the Yangtze Gorges area (fig. S5). One of reasons for this controversy is the uncertainty in the origin (autochthonous versus allochthonous) of the carbonate unit recording a positive CIE below the Miaohe Member (fig. S5). We emphasize that the two late Ediacaran negative CIEs (discussed below) proposed in this paper are not compromised by this stratigraphic uncertainty (see the Supplementary Materials). The date of 550.1 ± 0.6 Ma has been interpreted as the terminal timing either of the Shuram (*8*, *11*) or of a younger, post-Shuram CIE (*1*, *12*, *13*). These contrasting correlation models highlight the issues of regional complexity in developing regional chronostratigraphic frameworks; however (discussed below), the latter interpretation is preferred in this study. The Miaohe biota, preserved in the lower Miaohe Member and therefore older than ca. 550 Ma, is mainly composed of multicellular algae, putative metazoans, and problematica (*24*). Fossil assemblages of the Shibantan Member (Dengying Fm; Fig. 1) are dominated by soft-bodied Ediacara-type fossils (e.g., *Arborea*, *Dickinsonia*, *Pteridinium*, and *Rangea*), tubular fossils, vendotaenids, and trace fossils (*25*).

In the most proximal settings (eastern Yunnan Province; Fig. 1), the Shuram CIE occurs in the upper part of the Doushantuo Fm (*21*) and several hundred meters below ash beds in the Jiucheng Member (which contains the problematic tubular fossil *Shaanxilithes*) of the Dengying Fm with revised dates of 554.3 ± 0.6 Ma and 546.3 ± 0.7 Ma. The younger date is interpreted as a depositional age, while the interpretation of the older date reflects either reworking during deposition, incorporation of xenocrystic materials in the magmatic environment, or condensed deposition.

In slope settings in northeastern Guizhou Province, the black shale below the middle Doushantuo carbonate interval at the Wenghui section yields a new Re-Os date of 585.7 ± 2.8 Ma, providing a maximum age constraint on the Shuram CIE and the Wenghui biota (Fig. 1) (*26*). The highly radiogenic initial Os isotope composition ($^{187}Os/^{188}Os$ = 1.81) from the 585.7 ± 2.8–Ma isochron can be ascribed to either (i) deposition in a highly restricted basin (an explanation we consider unlikely given the depositional setting) or (ii) deposition in a euxinic water column with bottom-water sulfate concentrations high enough to sequester most of the unradiogenic hydrothermal-sourced Os into sulfides at the ridge before mixing with seawater (*27*). In more distal, deeper-water settings of southeastern Guizhou Province, the Doushantuo Fm is overlain by the Liuchapo Fm, which is composed predominantly of chert, with minor carbonate at the

base (Fig. 1). Ash beds from the carbonate and chert units of the Liuchapo Fm at Fanglong section were dated at 557 ± 3 Ma and 550 ± 3 Ma by SIMS zircon U-Pb method, respectively (*28*). In this study, ash beds from the topmost carbonate unit at the Wengxiu section (near the Xiajiaomeng section) and from the carbonate/chert contact at the Nangao section (*29*) are dated at 556.4 ± 0.7 Ma and 556.3 ± 0.7 Ma, respectively, by CA-ID-TIMS zircon U-Pb method (Fig. 1 and fig. S3). The three samples dated at ~557 to 556 Ma are all on a $\delta^{13}C_{carb}$ plateau of +1‰ and are all less than 10 m stratigraphically above the point at which a CIE recovery crosses 0‰ from a nadir of −8‰. In deeper water sections, the Shuram CIE is preserved in the uppermost part of the Doushantuo Fm (*3*), with recovery near the Doushantuo/Liuchapo boundary (*20*), corroborated by new $\delta^{13}C_{carb}$ data from Xiajiaomeng section (Fig. 1). The new dates demonstrate that the Liuchapo Fm is, in part, older than ca. 550 Ma and correlative with the upper Doushantuo Fm in the platform setting (Fig. 1), indicating a time-transgressive boundary between the Doushantuo and Dengying/Liuchapo Fms.

White Sea, East European Platform

The siliciclastic succession of the late Ediacaran Valdai Group in the White Sea area is composed of, from the bottom upward, the Lamtsa, Verkhovka, Zimnegory, and Erga Fms (Fig. 2). Abundant and diverse fossils are preserved in this succession from the upper Lamtsa Fm to the lower Erga Fm (*6*), forming the White Sea Ediacara-type fossil assemblage. Ash beds from the base of the Verkhovka Fm at the Agma River section and the Zimnegory Fm at the Zimnie Gory section yielded zircon U-Pb dates of 558 ± 1 Ma (*6*) and 555.3 ± 0.3 Ma (*30*), respectively. These two dates are refined here to 557.3 ± 0.6 Ma and 553.0 ± 0.7 Ma, providing high-precision age constraints on the White Sea assemblage. The first appearance datum of *Dickinsonia*, together with the oldest metazoan lipid biomarkers (*31*), is ca. 90 m below the 557.3 ± 0.6–Ma ash bed in the White Sea area. The oldest bilaterian body fossil *Kimberella*, a probable lophotrochozoan, occurs slightly above the 557.3 ± 0.6–Ma ash bed.

DISCUSSION

Number, duration, and synchroneity of 575- to 550-Ma CIEs

Radio-isotopic age constraints on the 575- to 550-Ma CIEs from South China, Oman, NW Canada, Namibia, and Brazil are summarized in Fig. 2. Examining the trends in $\delta^{13}C_{carb}$ within the constraints of our new radio-isotopic dates and their associated uncertainties and stratigraphic limitations allows the assessment of whether ca. 575- to 550-Ma $\delta^{13}C_{carb}$ excursions are globally correlative (Fig. 3). Moving systematically from platformal to slope-basinal settings in South China, at least one CIE older than 546.3 ± 0.7 Ma is present in the most proximal settings (eastern Yunnan Province), either one or two CIEs occur in platformal units in the Yangtze Gorge area, both are younger than 587.2 ± 3.6 Ma and terminated at 550 Ma ago, and one CIE occurs in basinal-slope settings (eastern Guizhou Province) constrained between 585.7 ± 2.8 Ma and 556.4 ± 0.7 Ma. In Oman, the Shuram CIE is constrained between 578.2 ± 5.9 Ma and 562.7 ± 3.8 Ma (*4*). In NW Canada, the Shuram CIE is older than 567.3 ± 3.0 Ma and younger than 574.0 ± 4.7 Ma (*4*). In Namibia, the basal Nama CIE ended before 547.4 ± 0.9 Ma (*10*) but with an inferred duration on the order of a few million years between that date and the end of the CIE based on co-occurrence of the CIE with weakly calcified metazoans (i.e., *Cloudina* and *Namacalathus*) and inferred inception of foredeep subsidence. In Brazil, the Tamengo Fm CIE is constrained between 555.2 ± 0.7 Ma and 542.4 ± 0.7 Ma (*32*).

Accepting all the interpretations outlined above, multiple large-magnitude negative CIEs can be proposed from ~575 Ma to 550 Ma (Fig. 3). Assuming that the largest CIEs that can be identified over considerable stratigraphic thicknesses in South China, Oman, and NW Canada are synchronous and represent a single correlative CIE (i.e., the Shuram CIE), we can infer that the Shuram CIE started after 574.0 ± 4.7 Ma and ended before 567.3 ± 3.0 Ma (*4*). This sustained negative CIE has also been reported from the Wonoka Fm in the Adelaide Geosyncline, Australia (*14*), the Patom Basin of southern Siberia (*33*), San Juan Fm of Peru (*34*), Johnnie Fm in Death Valley, USA (*35*), and Clemente Fm in NW Mexico (*36*). A younger and widespread CIE (*12*, *13*) is indicated by the termination of a CIE dated at 550.1 ± 0.6 Ma in South China, age constraints on the Tamengo CIE of Brazil, and the inferred termination of a negative CIE before 547.4 ± 0.9 Ma and likely at ~550 Ma in Namibia associated with *Cloudina* and *Namacalathus* (Fig. 3). The negative CIEs in the Stirling Quartzite of Death Valley (*35*), the lower Khatyspyt Fm of NE Siberia (*37*), the Zherba Fm of SE Siberia (*38*), and the middle Krol D of northern India (*39*) could also be correlative with this 550-Ma CIE, as they occur above where the Shuram CIE would be but below the Ediacaran-Cambrian boundary (Fig. 4).

The emerging view from this and previous studies (*1*, *4*, *12*, *13*) is that two globally expressed negative CIEs are recorded in 575- to 550-Ma strata and hence calls into question the traditional concept of a single sustained global CIE that terminated at ca. 550 Ma ago.

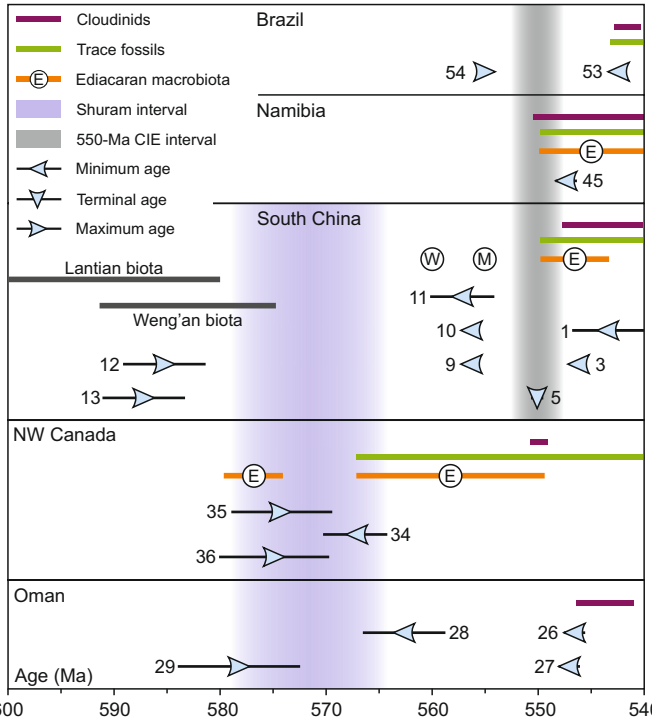

Fig. 3. Summary compilation of age constraints on late Ediacaran CIEs and comparison with fossil records. References to numbering of radio-isotopic ages are provided in table S5. The absence of the 550-Ma CIE in NW Canada and Oman may result from siliciclastic-dominated strata and/or depositional hiatuses. W, Wenghui biota; M, Miaohe biota.

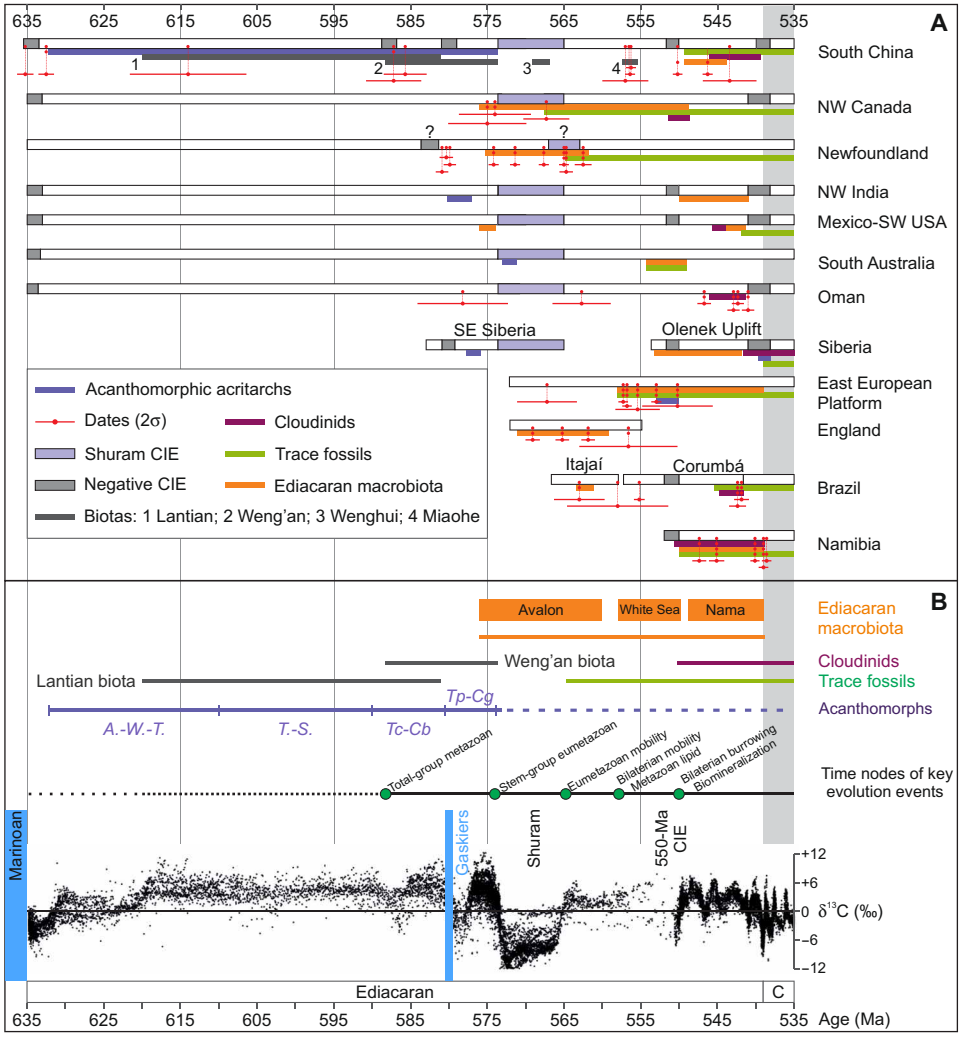

Fig. 4. Integrated radio-isotopic dates, fossil ranges, and carbon isotopic profile of the Ediacaran Period. (**A**) Sequences of Ediacaran fossils and $\delta^{13}C_{carb}$ profile pinned by radio-isotopic dates (table S5). Each radio-isotopic date is connected to its chemostratigraphic and/or paleontological context by red dot(s). The age uncertainty of ranges connected to radio-isotopic dates is constrained by the uncertainty of dates and the age difference between the dated horizon and the horizon of interest. Extra uncertainty associated with stratigraphic correlation needs to be considered for those ranges with no radio-isotopic dates connected. (**B**) Compiled $\delta^{13}C_{carb}$ profile for the Ediacaran Period and its comparison with fossil ranges. Avalon, White Sea, and Nama assemblages are presented as groupings solely on the basis of their current geographical settings. The evolutionary events (green dots) are based on fossil/biomarker records (see text for discussion). Compiled carbonate C isotopic data of 635- to 550-Ma interval are given in table S6. See the Supplementary Materials for discussion of the age ranges of the Lantian and Weng'an biota.

Maintaining the traditional concept requires considering additional and unrecognized sources of uncertainty to reconcile apparently conflicting constraints. Recent work combining the Re-Os and U-Pb geochronometers has further confirmed that application of the Re-Os system to organic-rich sedimentary rocks can yield ages comparable in accuracy to those provided by the U-Pb system (*40*). Uncertainties in radio-isotopic constraints and their interpretation as accurate depositional ages are sources of uncertainty to consider; however, the differences between the 567-Ma Re-Os and 550-Ma U-Pb dates are beyond those that can be reconciled through analytical errors or decay constant bias. An alternative perspective is to consider uncertainties in the interpretative framework used, namely, that the Shuram CIE represents a singular globally synchronous disturbance to the carbon cycle that could be correlated globally and would be similarly expressed in all basins. Although a full geochemical assessment of the drivers of large Neoproterozoic CIEs is beyond the scope of this work, the data provided here establish a framework in which Ediacaran CIEs could be global and correlative. Even if the Shuram CIE does not represent the global dissolved inorganic carbon (DIC) reservoir, it may be a coeval response of carbonate platforms globally to an external sea level or redox forcing (*41*). Depending on the drivers of the CIE(s), the magnitude of any given CIE may vary based on factors such as compositional variation associated with water depth, redox gradients, and processes internal to the carbonate platforms (*20*, *41*, *42*). Another issue to consider is differences in the shape of the CIE due to differential accumulation rates and/or incomplete preservation due to nondeposition and/or erosion. Hence, variable stratigraphic expression and difficulties in establishing precise correlation of late Ediacaran CIEs from region to region are not unexpected. Despite this uncertainty,

we note that the shape and magnitude of the Shuram CIE between disparate cratons (e.g., Siberian Platform, Laurentia, Arabia-Nubia, and Australia) are strikingly consistent in most sections when assuming near-constant regional sedimentation rates (*9*, *14*, *33*, *43*).

In Fig. 4, we apply both the direct age constraints on fossil assemblages and the newly proposed age model for late Ediacaran CIEs to construct a new age model for the Ediacaran fossil record. Despite the fact that we currently lack consensus regarding a mechanistic driver(s) for these CIEs and that we cannot demonstrate that these CIEs faithfully record the isotopic composition of the oceanic DIC pool, the two-CIE model presented here is consistent with the Shuram and 550-Ma CIEs being expressed on platform margins around the world (Fig. 4). This model is useful for both regional and global correlation, developing global chronostratigraphy and exploring causative processes for these Ediacaran CIEs.

A refined record of Ediacaran biotic evolution

The new Re-Os date of 587.2 ± 3.6 Ma from Hubei Province is near a second-order sequence boundary (for further discussions, see the Supplementary Materials) and thus provides a radio-isotopic age constraint for this stratigraphic package across the platform settings of South China (Fig. 1), which has substantial implications for the tempo of biotic evolution (*11*). First, it suggests that the maximum age of the Weng'an biota, which hosts diverse and complex multicellular organisms, is 587.2 ± 3.6 Ma (Fig. 1). Second, it serves as an age constraint for the boundary between the *T. tuberosum*–*S. zangwenlongii* and *T. conoideum*–*C. basiconica* microfossil assemblage zones, an important step in refining the Ediacaran biozones and its implication for stratigraphic correlation based on acanthomorphic acritarchs (Fig. 1; Supplementary Materials) (*17*). In more distal, deeper-water settings in northeastern Guizhou Province, the new Re-Os date of 585.7 ± 2.8 Ma provides a new maximum age constraint for the Wenghui biota characterized by diverse complex macroscopic carbonaceous fossils in the upper Doushantuo Fm (*26*). Together, these two dates facilitate correlation of fossil assemblages from the platform to the slope and demonstrate that lower Ediacaran strata are extremely condensed in South China.

Our new geochronological data provide the foundation for a refined global age model for the Ediacaran fossil record (Fig. 4). Early Ediacaran fossils are dominated by acanthomorphic species alongside macroalgae and putative animal fossils from the Lantian biota (*17*, *19*). After 587.2 ± 3.6 Ma, there is an increase in the abundance and diversity of the acanthomorphic species (*17*), accompanied by the diverse embryos that exhibit complex development probably hosting total-group metazoan, and putative microscopic metazoans (e.g., sponges) in the Weng'an biota (*18*, *44*). Macroscopic complex Ediacaran organisms made their first appearance between 580 and 574 Ma ago, whereas rangeomorphs (including some stem-group eumetazoans) diversified between 574 and 564 Ma ago through the Shuram CIE, and the oldest known record of eumetazoan mobility appeared 564.8 Ma ago (*45*). Diversification of nonrangeomorphs and increased evidence for bilaterian mobility, as exemplified by the White Sea assemblage, are constrained by U-Pb dates of 557.3 ± 0.6 Ma and 553.0 ± 0.7 Ma. Following the 550-Ma CIE and postulated first pulse of extinction (*46*) of Ediacaran taxa at the White Sea–Nama assemblage transition, skeletonized tubular fossils (cloudinids) and complex burrowing produced by bilaterian metazoans record the deep roots of the Cambrian explosion of metazoans alongside soft-bodied Ediacaran taxa (*25*).

Our age model presented for Ediacaran CIEs and fossil records provides the necessary chronometric context to test causal relationships, if any, between them. Independent of the drivers and global nature of the Ediacaran CIEs, the direct dates for Ediacaran fossil assemblages are a prerequisite for calibrating biostratigraphic records and improving the accuracy of molecular clock analysis to reconstruct the early evolutionary history of complex life. The emerging tempo of Ediacaran evolution is defined by assemblages of organisms with increasing ecosystem complexity that are relatively stable on tens of millions of year time scales, with new assemblages appearing across much shorter, discrete intervals (Fig. 4). At the current resolution, these transitions in the fossil record coincide with CIEs, suggestive of a potential causal relationship between environmental perturbations recorded in the carbon cycle and biological turnovers.

MATERIALS AND METHODS

U-Pb and Re-Os geochronology

Zircon grains were separated from each sample using conventional mineral separation techniques. They were pretreated by a chemical abrasion technique that involved thermal annealing in a furnace at 900°C for 60 hours, followed by partial dissolution in 29 M hydrofluoric acid (HF) at 180° to 210°C in high-pressure vessels for 12 hours. The chemically abraded grains were fluxed in/rinsed with several hundred microliters of 4 M HNO_3 and 6 M HCl to remove the leachates. All zircon fragments were spiked with the EARTHTIME ET535 (or ET2535) mixed isotopic tracer(s) (*47*, *48*) before complete dissolution in 29 M HF at 220°C for 60 hours and subsequent Pb and U purification by an HCl-based anion-exchange column chemistry.

Pb and U were loaded together onto single outgassed Re filaments along with a silica-gel emitter solution, and their isotopic ratios were measured on a Thermo Fisher Scientific Triton instrument equipped with an ion-counting SEM system. Pb was measured in dynamic mode on a MassCom secondary electron multiplier (SEM) and was corrected for mass bias using a fractionation factor of 0.12 ± 0.03%/amu (1σ) for samples prepared using the ET535 spike, and in real-time, based on measured $^{202}Pb/^{205}Pb$ ratios, for samples spiked with the ET2535 tracer. U isotopes were measured as dioxide ions either in static mode, on Faraday detectors equipped with 10^{12}-ohm resistors for intensities greater than 4 mV, or in dynamic mode for lower intensities. U mass fractionation was calculated in real time based on the isotopic composition of the ET535 and ET2535 tracers. Oxide correction was based on an $^{18}O/^{16}O$ ratio of 0.00205 ± 0.00004, and the sample $^{238}U/^{235}U$ ratio was assumed 137.818 ± 0.045 (*49*). Data reduction, calculation of dates, and propagation of uncertainties used the Tripoli and ET_Redux applications and algorithms (*50*).

Sampling and analytical procedures for Re-Os geochronology followed methods from (*51*, *52*) and are outlined briefly below. Any weathered surfaces were removed with a diamond-encrusted rock saw, and samples were then hand-polished using a diamond-encrusted polishing pad to remove cutting marks and eliminate any potential for contamination from the saw blade. The samples were dried overnight at 40°C and then crushed to a fine (~30 μm) powder in a SPEX 8500 Shatterbox using a zirconium grinding container and puck to homogenize any Re and Os heterogeneity present in the samples. Between 0.4 and 0.5 g of sample were digested and equilibrated in 8 ml of $Cr^{VI}O_3$-H_2SO_4 together with a mixed tracer (spike) solution of ^{190}Os and ^{185}Re in carius tubes at 220°C for 48 hours. Rhenium

and osmium were isolated and purified using solvent extraction [NaOH, $(CH_3)_2CO$, and $CHCl_3$], microdistillation, and anion column chromatography methods. The $Cr^{VI}O_3$-H_2SO_4 digestion method was used, as it has been shown to preferentially liberate hydrogenous Re and Os, yielding more accurate and precise age determinations (*40*, *52*). Total procedural blanks during this study were 61.3 ± 1.1 pg and 0.40 ± 0.17 pg for Re and Os, respectively, with an average $^{187}Os/^{188}Os$ value of 0.25 ± 0.8 (1σ, $n = 4$). The major source (>90%) of Re blank contamination is the $Cr^{VI}O_3$ used to make up the $Cr^{VI}O_3$-H_2SO_4 solution.

Isotopic measurements were performed using a Thermo Fisher Scientific TRITON PLUS mass spectrometer at Yale University, USA, via static Faraday collection for Re and ion counting using a secondary electron multiplier in peak-hopping mode for Os. The Os samples were loaded onto 99.995% Pt wire (H-Cross, NJ) in 9 N HBr, covered with a saturated solution of $Ba(OH)_2$ in 0.1 N NaOH as activator, and analyzed as oxides of Os. Interference of $^{187}ReO_3$ on $^{187}OsO_3$ was corrected by the measured intensity of $^{185}ReO_3$. Mass fractionation was corrected with $^{192}Os/^{188}Os = 3.0827$, using the exponential fractional law. Measurement quality was monitored by repeated measurement of the DROsS standard solution, which yielded $^{187}Os/^{188}Os$ of 0.16091 ± 0.00015 ($n = 12$) over the course of the measurement campaign for these samples. The Yale University Re standard solution (made from 99.999% Re wire, H-Cross, NJ, in 2 M HNO_3) measured on Faraday cups during analytical sessions yields an average $^{185}Re/^{187}Re$ value of 0.59811 ± 0.0006 (1σ, $n = 11$). The measured difference in $^{185}Re/^{187}Re$ values for the Re solution and the accepted $^{185}Re/^{187}Re$ value (0.59738) is used to correct the Re sample data for instrument mass fractionation and blank and spike contributions. Uncertainties for $^{187}Re/^{188}Os$ and $^{187}Os/^{188}Os$ were determined by error propagation of uncertainties in Re and Os mass spectrometry measurements, blank abundances and isotopic compositions, spike calibrations, and reproducibility of standard Re and Os isotopic values. The Re-Os isotopic data, 2-s calculated uncertainties for $^{187}Re/^{188}Os$ and $^{187}Os/^{188}Os$, and the associated error correlation function (rho) were regressed to yield a model 1 Re-Os date using Isoplot V.4.15 with the λ ^{187}Re constant of 1.666×10^{-11} a^{-1} (*53*).

Carbonate carbon and oxygen isotopes

Carbonate powders were drilled from freshly cut rock slab surfaces using a dental drill for carbon and oxygen isotope analysis. Fine-grained micrites were preferentially selected. The obtained powders were reacted with 100% phosphoric acid at 70°C and were analyzed for carbon and oxygen isotopes using a Kiel IV device connected to a Finnigan MAT 253 mass spectrometer at the Nanjing Institute of Geology and Palaeontology, Chinese Academy of Sciences. Reproducibility was better than ±0.03‰ and ±0.08‰ (1 SD) for carbon and oxygen isotopes. All analyses were calibrated to the Chinese National Standard (GBW-04405), an Ordovician carbonate from a site near Beijing, with a $\delta^{13}C_{carb}$ value of +0.57‰ and a $\delta^{18}O_{carb}$ value of −8.49‰. All data are given in per mil (‰) relative to Vienna-Pee Dee Belemnite.

Integration of Ediacaran fossil and carbonate carbon isotopic records

The integration of global Ediacaran fossil and $\delta^{13}C_{carb}$ records to produce Fig. 4 (A and B) was based on a combination of regional bio- and chemostratigraphic records. Integration of these regional records was facilitated by the temporal constraints imposed by the radio-isotopic dates, with additional correlation using first-order regional bio- and chemostratigraphic features. The main challenge of this work is how to deal with the intervals with no absolute age constraints. Our approach has (illustrated in Fig. 4A) been to use the best constrained regions to provide the age calibration of a given feature (i.e., CIE), and then, in the regions where the feature is "floating," it is given the age from the best calibrated region. Where not directly dated, the age range of fossil assemblage/biota is defined by estimated age difference between the dated horizon and the horizon of interest and its stratigraphic position relative to $\delta^{13}C_{carb}$ CIE(s). Age ranges of Ediacaran fossil assemblages and biotas are discussed in the main text and the Supplementary Materials. We note that these intervals that lack constraint from radio-isotopic dates are considered the most uncertain, and extra uncertainty associated with stratigraphic correlation (the assumptions underpinned) needs to be considered when integrating the records into a global framework. The time nodes of key evolutionary events in Fig. 4B are tied to key fossil assemblages that are discussed in the main text. As these nodes are based on the fossil record, they are minimum age constraints for the inferred biological innovation.

We have compiled published high-resolution $\delta^{13}C_{carb}$ data from >150 globally distributed Ediacaran sections (Australia, Brazil, Mongolia, Namibia, USA, Canada, Oman, South China, and Siberia). In each case, data are first correlated regionally by combined litho-, chemo-, and sequence stratigraphy. Gaps in the $\delta^{13}C_{carb}$ record of individual sections are permitted at unconformities, exposure surfaces, or during intervals of siliciclastic or evaporitic deposition. We prioritize $\delta^{13}C_{carb}$ records for sections that include interbedded radio-isotopic constraints from zircon CA-ID-TIMS U-Pb and black-shale Re-Os geochronology. $\delta^{13}C_{carb}$ values that are anchored by the age of each tuff deposit or Re-Os age provide the scaffold for wider correlation. Intervals that lack age constraints are considered the most uncertain and are correlated through $\delta^{13}C_{carb}$ trends. We start our correlation at 635 Ma, where marine sediments record deglaciation from the global Marinoan cryochron (*8*). This approach produces a new global composite $\delta^{13}C$ curve (Fig. 4B) consistent with available geochronological information.

SUPPLEMENTARY MATERIALS

Supplementary material for this article is available at https://science.org/doi/10.1126/sciadv.abi9643

REFERENCES AND NOTES

1. S. H. Xiao, G. M. Narbonne, *The Ediacaran Period* (Elsevier B.V., 2020).
2. P. F. Hoffman, D. S. Abbot, Y. Ashkenazy, D. I. Benn, J. J. Brocks, P. A. Cohen, G. M. Cox, J. R. Creveling, Y. Donnadieu, D. H. Erwin, I. J. Fairchild, D. Ferreira, J. C. Goodman, G. P. Halverson, M. F. Jansen, G. Le Hir, G. D. Love, F. A. Macdonald, A. C. Maloof, C. A. Partin, G. Ramstein, B. E. J. Rose, C. V. Rose, P. M. Sadler, E. Tziperman, A. Voigt, S. G. Warren, Snowball Earth climate dynamics and Cryogenian geology-geobiology. *Sci. Adv.* **3**, e1600983 (2017).
3. M. Lu, M. Zhu, J. Zhang, G. Shields-Zhou, G. Li, F. Zhao, X. Zhao, M. Zhao, The DOUNCE event at the top of the Ediacaran Doushantuo Formation, South China: Broad stratigraphic occurrence and non-diagenetic origin. *Precambrian Res.* **225**, 86–109 (2013).
4. A. D. Rooney, M. D. Cantine, K. D. Bergmann, I. Gómez-Pérez, B. Al Baloushi, T. H. Boag, J. F. Busch, E. A. Sperling, J. V. Strauss, Calibrating the coevolution of Ediacaran life and environment. *Proc. Natl. Acad. Sci. U.S.A.* **117**, 16824–16830 (2020).
5. J. P. Pu, S. A. Bowring, J. Ramezani, P. Myrow, T. D. Raub, E. Landing, A. Mills, E. Hodgin, F. A. Macdonald, Dodging snowballs: Geochronology of the Gaskiers glaciation and the first appearance of the Ediacaran biota. *Geology* **44**, 955–958 (2016).
6. D. Grazhdankin, Patterns of distribution in the Ediacaran biotas: Facies versus biogeography and evolution. *Paleobiology* **30**, 203–221 (2004).
7. J. G. Gehling, M. L. Droser, How well do fossil assemblages of the Ediacara Biota tell time? *Geology* **41**, 447–450 (2013).

8. D. Condon, M. Zhu, S. Bowring, W. Wang, A. Yang, Y. Jin, U-Pb ages from the Neoproterozoic Doushantuo Formation, China. *Science* **308**, 95–98 (2005).
9. E. Le Guerroué, P. A. Allen, A. Cozzi, J. L. Etienne, M. Fanning, 50 Myr recovery from the largest negative $\delta^{13}C$ excursion in the Ediacaran ocean. *Terra Nova* **18**, 147–153 (2006).
10. S. A. Bowring, J. P. Grotzinger, D. J. Condon, J. Ramezani, M. J. Newall, P. A. Allen, Geochronologic constraints on the chronostratigraphic framework of the Neoproterozoic Huqf Supergroup, Sultanate of Oman. *Am. J. Sci.* **307**, 1097–1145 (2007).
11. M. Zhu, M. Lu, J. Zhang, F. Zhao, G. Li, Y. Aihua, X. Zhao, M. Zhao, Carbon isotope chemostratigraphy and sedimentary facies evolution of the Ediacaran Doushantuo Formation in western Hubei, South China. *Precambrian Res.* **225**, 7–28 (2013).
12. Z. An, G. Jiang, J. Tong, L. Tian, Q. Ye, H. Song, H. Song, Stratigraphic position of the Ediacaran Miaohe biota and its constrains on the age of the upper Doushantuo $\delta^{13}C$ anomaly in the Yangtze Gorges area, South China. *Precambrian Res.* **271**, 243–253 (2015).
13. C. Zhou, S. Xiao, W. Wang, C. Guan, Q. Ouyang, Z. Chen, The stratigraphic complexity of the middle Ediacaran carbon isotopic record in the Yangtze Gorges area, South China, and its implications for the age and chemostratigraphic significance of the Shuram excursion. *Precambrian Res.* **288**, 23–38 (2017).
14. J. M. Husson, J. A. Higgins, A. C. Maloof, B. Schoene, Ca and Mg isotope constraints on the origin of Earth's deepest $\delta^{13}C$ excursion. *Geochim. Cosmochim. Acta* **160**, 243–266 (2015).
15. G. A. Shields, B. J. W. Mills, M. Zhu, T. D. Raub, S. J. Daines, T. M. Lenton, Unique Neoproterozoic carbon isotope excursions sustained by coupled evaporite dissolution and pyrite burial. *Nat. Geosci.* **12**, 823–827 (2019).
16. M. Zhu, X. H. Li, Introduction: From snowball Earth to the Cambrian explosion-evidence from China. *Geol. Mag.* **154**, 1187–1192 (2017).
17. P. Liu, M. Moczydłowska, *Ediacaran Microfossils from the Doushantuo Formation Chert Nodules in the Yangtze Gorges Area, South China, and New Biozones* (John Wiley & Sons Ltd., 2019).
18. S. Xiao, A. D. Muscente, L. Chen, C. Zhou, J. D. Schiffbauer, A. D. Wood, N. F. Polys, X. Yuan, The Weng'an biota and the Ediacaran radiation of multicellular eukaryotes. *Natl. Sci. Rev.* **1**, 498–520 (2014).
19. X. Yuan, Z. Chen, S. Xiao, C. Zhou, H. Hua, An early Ediacaran assemblage of macroscopic and morphologically differentiated eukaryotes. *Nature* **470**, 390–393 (2011).
20. G. Jiang, A. J. Kaufman, N. Christie-Blick, S. Zhang, H. Wu, Carbon isotope variability across the Ediacaran Yangtze platform in South China: Implications for a large surface-to-deep ocean $\delta^{13}C$ gradient. *Earth Planet. Sci. Lett.* **261**, 303–320 (2007).
21. M. Zhu, J. Zhang, A. Yang, Integrated Ediacaran (Sinian) chronostratigraphy of South China. *Palaeogeogr. Palaeoclimatol. Palaeoecol.* **254**, 7–61 (2007).
22. C. Zhou, X. Li, S. Xiao, Z. Lan, Q. Ouyang, C. Guan, Z. Chen, A new SIMS zircon U–Pb date from the Ediacaran Doushantuo Formation: Age constraint on the Weng'an biota. *Geol. Mag.* **154**, 1193–1201 (2017).
23. Q. Ouyang, C. Zhou, S. Xiao, Z. Chen, Y. Shao, Acanthomorphic acritarchs from the Ediacaran Doushantuo Formation at Zhangcunping in South China, with implications for the evolution of early Ediacaran eukaryotes. *Precambrian Res.* **320**, 171–192 (2019).
24. Q. Ye, J. Tong, Z. An, J. Hu, L. Tian, K. Guan, S. Xiao, A systematic description of new macrofossil material from the upper Ediacaran Miaohe Member in South China. *J. Syst. Palaeontol.* **17**, 183–238 (2019).
25. S. Xiao, Z. Chen, K. Pang, C. Zhou, X. Yuan, The Shibantan lagerstätte: Insights into the Proterozoic–Phanerozoic transition. *J. Geol. Soc. London* **178**, jgs2020-135 (2020).
26. M. Zhu, J. G. Gehling, S. Xiao, Y. Zhao, M. L. Droser, Eight-armed Ediacara fossil preserved in contrasting taphonomic windows from China and Australia. *Geology* **36**, 867–870 (2008).
27. D. D. Syverson, J. A. R. Katchinoff, L. R. Yohe, B. M. Tutolo, W. E. Seyfried Jr., A. D. Rooney, Experimental partitioning of osmium between pyrite and fluid: Constraints on the mid-ocean ridge hydrothermal flux of osmium to seawater. *Geochim. Cosmochim. Acta* **293**, 240–255 (2021).
28. M. Zhou, T. Luo, W. D. Huff, Z. Yang, G. Zhou, T. Gan, H. Yang, D. Zhang, Timing the termination of the Doushantuo negative carbon isotope excursion: Evidence from U-Pb ages from the Dengying and Liuchapo formations, South China. *Sci. Bull.* **63**, 1431–1438 (2018).
29. X. L. Yang, M. Y. Zhu, Q. J. Guo, Y. L. Zhao, Organic carbon isotopic evolution during the Ediacaran-Cambrian transition interval in eastern Guizhou, South China: Paleoenvironmental and stratigraphic implications. *Acta Geol. Sin. Engl.* **81**, 194–203 (2007).
30. M. W. Martin, D. V. Grazhdankin, S. A. Bowring, D. A. D. Evans, M. A. Fedonkin, J. L. Kirschvink, Age of Neoproterozoic bilatarian body and trace fossils, White Sea, Russia: Implications for metazoan evolution. *Science* **288**, 841–845 (2000).
31. I. Bobrovskiy, J. M. Hope, A. Ivantsov, B. J. Nettersheim, C. Hallmann, J. J. Brocks, Ancient steroids establish the Ediacaran fossil *Dickinsonia* as one of the earliest animals. *Science* **361**, 1246–1249 (2018).
32. L. A. Parry, P. C. Boggiani, D. J. Condon, R. J. Garwood, J. D. M. Leme, D. McIlroy, M. D. Brasier, R. Trindade, G. A. C. Campanha, M. L. A. F. Pacheco, C. Q. C. Diniz, A. G. Liu, Ichnological evidence for meiofaunal bilaterians from the terminal Ediacaran and earliest Cambrian of Brazil. *Nat. Ecol. Evol.* **1**, 1455–1464 (2017).
33. V. A. Melezhik, B. G. Pokrovsky, A. E. Fallick, A. B. Kuznetsov, M. I. Bujakaite, Constraints on $^{87}Sr/^{86}Sr$ of late Ediacaran seawater: Insight from Siberian high-Sr limestones. *J. Geol. Soc. Lond.* **166**, 183–191 (2009).
34. E. Hodgin, thesis, Harvard University (2020).
35. C. Verdel, B. P. Wernicke, S. A. Bowring, The Shuram and subsequent Ediacaran carbon isotope excursions from southwest Laurentia, and implications for environmental stability during the metazoan radiation. *GSA Bull.* **123**, 1539–1559 (2011).
36. Z. Li, M. Cao, S. J. Loyd, T. J. Algeo, H. Zhao, X. Wang, L. Zhao, Z.-Q. Q. Chen, Transient and stepwise ocean oxygenation during the late Ediacaran Shuram Excursion: Insights from carbonate $\delta^{238}U$ of northwestern Mexico. *Precambrian Res.* **344**, 105741 (2020).
37. H. Cui, D. V. Grazhdankin, S. Xiao, S. Peek, V. I. Rogov, N. V. Bykova, N. E. Sievers, X. M. Liu, A. J. Kaufman, Redox-dependent distribution of early macro-organisms: Evidence from the terminal Ediacaran Khatyspyt Formation in Arctic Siberia. *Palaeogeogr. Palaeoclimatol. Palaeoecol.* **461**, 122–139 (2016).
38. S. M. Pelechaty, Integrated chronostratigraphy of the Vendian System of Siberia: Implications for a global stratigraphy. *J. Geol. Soc.* **155**, 957–973 (1998).
39. A. J. Kaufman, G. Jiang, N. Christie-Blick, D. M. Banerjee, V. Rai, Stable isotope record of the terminal Neoproterozoic Krol platform in the Lesser Himalayas of northern India. *Precambrian Res.* **147**, 156–185 (2006).
40. A. D. Rooney, C. Yang, D. J. Condon, M. Zhu, F. A. Macdonald, U-Pb and Re-Os geochronology tracks stratigraphic condensation in the Sturtian snowball Earth aftermath. *Geology* **48**, 625–629 (2020).
41. A.-S. C. Ahm, A. C. Maloof, F. A. Macdonald, P. F. Hoffman, C. J. Bjerrum, U. Bold, C. V. Rose, J. V. Strauss, J. A. Higgins, An early diagenetic deglacial origin for basal Ediacaran "cap dolostones". *Earth Planet. Sci. Lett.* **506**, 292–307 (2019).
42. E. C. Geyman, A. C. Maloof, A diurnal carbon engine explains ^{13}C-enriched carbonates without increasing the global production of oxygen. *Proc. Natl. Acad. Sci. U.S.A.* **116**, 24433–24439 (2019).
43. D. P. Moynihan, J. V. Strauss, L. L. Nelson, C. D. Padget, Upper Windermere Supergroup and the transition from rifting to continent-margin sedimentation, Nadaleen River area, northern Canadian Cordillera. *GSA Bull.* **131**, 1673–1701 (2019).
44. Z. Yin, M. Zhu, E. H. Davidson, D. J. Bottjer, F. Zhao, P. Tafforeau, Sponge grade body fossil with cellular resolution dating 60 Myr before the Cambrian. *Proc. Natl. Acad. Sci. U.S.A.* **112**, E1453–E1460 (2015).
45. J. J. Matthews, A. G. Liu, C. Yang, D. McIlroy, B. Levell, D. J. Condon, A chronostratigraphic framework for the rise of the ediacaran macrobiota: New constraints from mistaken point ecological reserve, Newfoundland. *GSA Bull.* **133**, 612–624 (2021).
46. S. A. F. Darroch, E. F. Smith, M. Laflamme, D. H. Erwin, Ediacaran extinction and cambrian explosion. *Trends Ecol. Evol.* **33**, 653–663 (2018).
47. D. J. Condon, B. Schoene, N. M. McLean, S. A. Bowring, R. R. Parrish, Metrology and traceability of U-Pb isotope dilution geochronology (EARTHTIME Tracer Calibration Part I). *Geochim. Cosmochim. Acta* **164**, 464–480 (2015).
48. N. M. McLean, D. J. Condon, B. Schoene, S. A. Bowring, Evaluating uncertainties in the calibration of isotopic reference materials and multi-element isotopic tracers (EARTHTIME Tracer Calibration Part II). *Geochim. Cosmochim. Acta* **164**, 481–501 (2015).
49. J. Hiess, D. J. Condon, N. McLean, S. R. Noble, $^{238}U/^{235}U$ systematics in terrestrial uranium-bearing minerals. *Science* **335**, 1610–1614 (2012).
50. N. M. McLean, J. F. Bowring, S. A. Bowring, An algorithm for U-Pb isotope dilution data reduction and uncertainty propagation. *Geochem. Geophys. Geosysts.* **12**, Q0AA18 (2011).
51. J. V. Strauss, A. D. Rooney, F. A. MacDonald, A. D. Brandon, A. H. Knoll, 740 Ma vase-shaped microfossils from Yukon, Canada: Implications for neoproterozoic chronology and biostratigraphy. *Geology* **42**, 659–662 (2014).
52. D. Selby, R. A. Creaser, Re-Os geochronology of organic rich sediments: An evaluation of organic matter analysis methods. *Chem. Geol.* **200**, 225–240 (2003).
53. M. I. Smoliar, R. J. Walker, J. W. Morgan, Re-Os ages of group IIA, IIIA, IVA, and IVB iron meteorites. *Science* **271**, 1099–1102 (1996).
54. D. Li, H.-F. Ling, G. A. Shields-Zhou, X. Chen, L. Cremonese, L. Och, M. Thirlwall, C. J. Manning, Carbon and strontium isotope evolution of seawater across the Ediacaran–Cambrian transition: Evidence from the Xiaotan section, NE Yunnan, South China. *Precambrian Res.* **225**, 128–147 (2013).
55. Z. Wang, J. Wang, E. Suess, G. Wang, C. Chen, S. Xiao, Silicified glendonites in the Ediacaran Doushantuo Formation (South China) and their potential paleoclimatic implications. *Geology* **45**, 115–118 (2017).
56. M. Zhu, A. Yang, X. Yang, J. Peng, J. Zhang, M. Lu, Ediacaran succession and the Wenghui Biota in the deep-water facies of the Yangtze Platform at Wenghui, Jiangkou County, Guizhou. *J. Guizhou Univ. (Natural Sci.)* **29**, 133–138 (2012).

57. P. Liu, C. Yin, L. Gao, F. Tang, S. Chen, New material of microfossils from the Ediacaran Doushantuo Formation in the Zhangcunping area, Yichang, Hubei Province and its zircon SHRIMP U-Pb age. *Chin. Sci. Bull.* **54**, 1058–1064 (2009).
58. R. A. Wood, S. W. Poulton, A. R. Prave, K. H. Hoffmann, M. O. Clarkson, R. Guilbaud, J. W. Lyne, R. Tostevin, F. Bowyer, A. M. Penny, A. Curtis, S. A. Kasemann, Dynamic redox conditions control late Ediacaran metazoan ecosystems in the Nama Group, Namibia. *Precambrian Res.* **261**, 252–271 (2015).
59. P. C. Boggiani, C. Gaucher, A. N. Sial, M. Babinski, C. M. Simon, C. Riccomini, V. P. Ferreira, T. R. Fairchild, Chemostratigraphy of the Tamengo Formation (Corumbá Group, Brazil): A contribution to the calibration of the Ediacaran carbon-isotope curve. *Precambrian Res.* **182**, 382–401 (2010).
60. K. A. McFadden, J. Huang, X. Chu, G. Jiang, A. J. Kaufman, C. Zhou, X. Yuan, S. Xiao, Pulsed oxidation and biological evolution in the Ediacaran Doushantuo Formation. *Proc. Natl. Acad. Sci. U.S.A.* **105**, 3197–3202 (2008).
61. G. H. Barfod, F. Albarède, A. H. Knoll, S. Xiao, P. Télouk, R. Frei, J. Baker, New Lu-Hf and Pb-Pb age constraints on the earliest animal fossils. *Earth Planet. Sci. Lett.* **201**, 203–212 (2002).
62. Y. Sui, C. Huang, R. Zhang, Z. Wang, J. Ogg, D. B. Kemp, Astronomical time scale for the lower Doushantuo Formation of early Ediacaran, South China. *Sci. Bull.* **63**, 1485–1494 (2018).
63. B. Zhu, H. Becker, S.-Y. Jiang, D.-H. Pi, M. Fischer-Gödde, J. H. Yang, Re–Os geochronology of black shales from the Neoproterozoic Doushantuo Formation, Yangtze platform, South China. *Precambrian Res.* **225**, 67–76 (2013).
64. A. D. Rooney, D. Selby, J.-P. Houzay, P. R. Renne, Re–Os geochronology of a Mesoproterozoic sedimentary succession, Taoudeni basin, Mauritania: Implications for basin-wide correlations and Re–Os organic-rich sediments systematics. *Earth Planet. Sci. Lett.* **289**, 486–496 (2010).
65. W. Wang, C. Guan, C. Zhou, Y. Peng, L. M. Pratt, X. Chen, L. Chen, Z. Chen, X. Yuan, S. Xiao, Integrated carbon, sulfur, and nitrogen isotope chemostratigraphy of the Ediacaran Lantian Formation in South China: Spatial gradient, ocean redox oscillation, and fossil distribution. *Geobiology* **15**, 552–571 (2017).
66. M. Tahata, Y. Ueno, T. Ishikawa, Y. Sawaki, K. Murakami, J. Han, D. Shu, Y. Li, J. Guo, N. Yoshida, T. Komiya, Carbon and oxygen isotope chemostratigraphies of the Yangtze platform, South China: Decoding temperature and environmental changes through the Ediacaran. *Gondw. Res.* **23**, 333–353 (2013).
67. D. E. Canfield, A. H. Knoll, S. W. Poulton, G. M. Narbonne, G. R. Dunning, Carbon isotopes in clastic rocks and the Neoproterozoic carbon cycle. *Am. J. Sci.* **320**, 97–124 (2020).
68. E. Vernhet, C. Heubeck, M. Y. Zhu, J. M. Zhang, Stratigraphic reconstruction of the Ediacaran Yangtze platform margin (Hunan province, China) using a large olistolith. *Palaeogeogr. Palaeoclimatol. Palaeoecol.* **254**, 123–139 (2007).
69. X. Chen, P. Zhou, B. Zhang, C. Wang, Stable isotope records of the Ediacaran Doushantuo Formation in the eastern Yangtze Gorges and its significance for choronostratigraphy. *Geol. China* **42**, 207–223 (2015).
70. C. Yang, X. H. Li, M. Zhu, D. J. Condon, SIMS U–Pb zircon geochronological constraints on upper Ediacaran stratigraphic correlations, South China. *Geol. Mag.* **154**, 1202–1216 (2017).
71. A. H. Jaffey, K. F. Flynn, L. E. Glendenin, W. C. Bentley, A. M. Essling, Precision measurement of half-lives and specific activities of ^{235}U and ^{238}U. *Phys. Rev. C* **4**, 1889–1906 (1971).
72. T. Huang, D. Chen, Y. Ding, X. Zhou, G. Zhang, SIMS U-Pb zircon geochronological and carbon isotope chemostratigraphic constraints on the Ediacaran-Cambrian boundary succession in the three gorges area, south China. *J. Earth Sci.* **31**, 69–78 (2020).
73. C. Yang, M. Zhu, D. J. Condon, X. H. Li, Geochronological constraints on stratigraphic correlation and oceanic oxygenation in Ediacaran-Cambrian transition in South China. *J. Asian Earth Sci.* **140**, 75–81 (2017).
74. C. Chen, Q. Feng, Z. Gan, Zircon U-Pb ages and its geological significance of tuffs between Doushantuo and Liuchapo formations at Yangtou Section, Guizhou Province. *Earth Sci.* **45**, 880–891 (2020).
75. J. E. Amthor, J. P. Grotzinger, S. Schröder, S. A. Bowring, J. Ramezani, M. W. Martin, A. Matter, Extinction of Cloudina and Namacalathus at the Precambrian-Cambrian boundary in Oman. *Geology* **31**, 431–434 (2003).
76. M. Brasier, G. McCarron, R. Tucker, J. Leather, P. Allen, G. Shields, New U-Pb zircon dates for the Neoproterozoic Ghubrah glaciation and for the top of the Huqf Supergroup, Oman. *Geology* **28**, 175–178 (2000).
77. A. D. Rooney, J. V. Strauss, A. D. Brandon, F. A. Macdonald, A Cryogenian chronology: Two long-lasting synchronous neoproterozoic glaciations. *Geology* **43**, 459–462 (2015).
78. U. Linnemann, M. Ovtcharova, U. Schaltegger, A. Gärtner, M. Hautmann, G. Geyer, P. Vickers-Rich, T. Rich, B. Plessen, M. Hofmann, J. Zieger, R. Krause, L. Kriesfeld, J. Smith, New high-resolution age data from the Ediacaran–Cambrian boundary indicate rapid, ecologically driven onset of the Cambrian explosion. *Terra Nova* **31**, 49–58 (2019).
79. J. P. Grotzinger, S. A. Bowring, B. Z. Saylor, A. J. Kaufman, Biostratigraphic and geochronologic constraints on early animal evolution. *Science* **270**, 598–604 (1995).
80. A. R. Prave, D. J. Condon, K. H. Hoffmann, S. Tapster, A. E. Fallick, Duration and nature of the end-Cryogenian (Marinoan) glaciation. *Geology* **44**, 631–634 (2016).
81. K. H. Hoffmann, D. J. Condon, S. A. Bowring, J. L. Crowley, U-Pb zircon date from the Neoproterozoic Ghaub Formation Namibia: Constraints on Marinoan glaciation. *Geology* **32**, 817–820 (2004).
82. M. A. S. Basei, C. O. Drukas, A. P. Nutman, K. Wemmer, L. Dunyi, P. R. Santos, C. R. Passarelli, M. C. C. Neto, O. Siga Jr., L. Osako, The Itajaí foreland basin: A tectono-sedimentary record of the Ediacaran period, Southern Brazil. *Int. J. Earth Sci.* **100**, 543–569 (2011).
83. B. Becker-Kerber, P. S. G. Paim, F. Chemale Junior, T. J. Girelli, A. L. Z. da Rosa, A. El Albani, G. L. Osés, G. M. E. M. Prado, M. Figueiredo, L. S. A. Simões, M. L. A. F. Pacheco, The oldest record of Ediacaran macrofossils in Gondwana (~563 Ma, Itajaí Basin, Brazil). *Gondw. Res.* **84**, 211–228 (2020).
84. S. R. Noble, D. J. Condon, J. N. Carney, P. R. Wilby, T. C. Pharaoh, T. D. Ford, U–Pb geochronology and global context of the charnian supergroup, UK: Constraints on the age of key Ediacaran fossil assemblages. *GSA Bull.* **127**, 250–265 (2015).
85. M. P. I. Llanos, J. A. Tait, V. Popov, A. Abalmassova, Palaeomagnetic data from Ediacaran (Vendian) sediments of the Arkhangelsk region, NW Russia: An alternative apparent polar wander path of Baltica for the Late Proterozoic-Early Palaeozoic. *Earth Planet. Sci. Lett.* **240**, 732–747 (2005).
86. Y. Soldatenko, A. El Albani, M. Ruzina, C. Fontaine, V. Nesterovsky, J. L. Paquette, A. Meunier, M. Ovtcharova, Precise U-Pb age constrains on the Ediacaran biota in Podolia, East European Platform, Ukraine. *Sci. Rep.* **9**, 1675 (2019).
87. D. V. Grazhdankin, V. V. Marusin, J. Meert, M. T. Krupenin, A. V. Maslov, Kotlin regional stage in the South Urals. *Dokl. Earth Sci.* **440**, 1222–1226 (2011).
88. S. A. Bowring, J. P. Grotzinger, C. E. Isachsen, A. H. Knoll, S. M. Pelechaty, P. Kolosov, Calibrating rates of early Cambrian evolution. *Science* **261**, 1293–1298 (1993).
89. C. R. Calver, Isotope stratigraphy of the Ediacarian (Neoproterozoic III) of the Adelaide Rift Complex, Australia, and the overprint of water column stratification. *Precambrian Res.* **100**, 121–150 (2000).
90. J. M. Husson, A. C. Maloof, B. Schoene, C. Y. Chen, J. A. Higgins, Stratigraphic expression of Earth's deepest δ^{13}C excursion in the wonoka formation of South Australia. *Am. J. Sci.* **315**, 1–45 (2015).
91. X. Wang, G. Jiang, X. Shi, S. Xiao, Paired carbonate and organic carbon isotope variations of the Ediacaran Doushantuo Formation from an upper slope section at Siduping, South China. *Precambrian Res.* **273**, 53–66 (2016).
92. C. Zhou, S. Jiang, S. Xiao, Z. Chen, X. Yuan, Rare earth elements and carbon isotope geochemistry of the Doushantuo Formation in South China: Implication for middle Ediacaran shallow marine redox conditions. *Chin. Sci. Bull.* **57**, 1998–2006 (2012).
93. W. Wang, C. Zhou, C. Guan, X. Yuan, Z. Chen, B. Wan, An integrated carbon, oxygen, and strontium isotopic studies of the Lantian Formation in South China with implications for the Shuram anomaly. *Chem. Geol.* **373**, 10–26 (2014).
94. F. A. Macdonald, J. V. Strauss, E. A. Sperling, G. P. Halverson, G. M. Narbonne, D. T. Johnston, M. Kunzmann, D. P. Schrag, J. A. Higgins, The stratigraphic relationship between the Shuram carbon isotope excursion, the oxygenation of Neoproterozoic oceans, and the first appearance of the Ediacara biota and bilaterian trace fossils in northwestern Canada. *Chem. Geol.* **362**, 250–272 (2013).
95. U. Bold, E. F. Smith, A. D. Rooney, S. A. Bowring, R. Buchwaldt, F. O. Dudás, J. Ramezani, J. L. Crowley, D. P. Schrag, F. A. Macdonald, Neoproterozoic stratigraphy of the zavkhan terrane of Mongolia: The backbone for cryogenian and early ediacaran chemostratigraphic records. *Am. J. Sci.* **315**, 1–63 (2016).
96. B. Z. Saylor, A. J. Kaufman, J. P. Grotzinger, F. Urban, A composite reference section for terminal proterozoic strata of Southern Namibia. *J. Sediment. Res.* **68**, 1223–1235 (1998).
97. B. Z. Saylor, thesis, Massachusetts Institute of Technology (1996).
98. G. P. Halverson, P. F. Hoffman, D. P. Schrag, A. C. Maloof, A. H. N. Rice, Toward a Neoproterozoic composite carbon-isotope record. *GSA Bull.* **117**, 1181–1207 (2005).
99. D. A. Fike, J. P. Grotzinger, A paired sulfate-pyrite δ^{34}S approach to understanding the evolution of the Ediacaran-Cambrian sulfur cycle. *Geochim. Cosmochim. Acta* **72**, 2636–2648 (2008).
100. D. A. Fike, J. P. Grotzinger, L. M. Pratt, R. E. Summons, Oxidation of the Ediacaran ocean. *Nature* **444**, 744–747 (2006).
101. P. A. Allen, J. Leather, M. D. Brasier, The Neoproterozoic Fiq glaciation and its aftermath, Huqf supergroup of Oman. *Basin Res.* **16**, 507–534 (2004).
102. M. R. Osburn, J. Owens, K. D. Bergmann, T. W. Lyons, J. P. Grotzinger, Dynamic changes in sulfate sulfur isotopes preceding the Ediacaran Shuram Excursion. *Geochim. Cosmochim. Acta* **170**, 204–224 (2015).
103. M. R. Osburn, thesis, California Institute of Technology (2013).
104. B. G. Pokrovsky, M. I. Bujakaite, O. V. Kokin, Geochemistry of C, O, and Sr isotopes and chemostratigraphy of neoproterozoic rocks in the northern Yenisei Ridge. *Lithol. Miner. Resour.* **47**, 177–199 (2012).

105. B. G. Pokrovskii, V. A. Melezhik, M. I. Bujakaite, Carbon, oxygen, strontium, and sulfur isotopic compositions in late Precambrian rocks of the Patom Complex, central Siberia: Communication 1. results, isotope stratigraphy, and dating problems. *Lithol. Miner. Resour.* **41**, 450–474 (2006).
106. M. A. Semikhatov, A. B. Kuznetsov, V. N. Podkovyrov, J. K. Bartley, Y. V. Davydov, The Yudoma Group of stratotype area: C-isotope chemostratigraphic correlations and Yudomian-Vendian relation. *Stratigr. Geol. Correl.* **12**, 435–459 (2004).
107. M. Lu, M. Zhu, F. Zhao, Revisiting the Tianjiayuanzi section-the stratotype section of the Edoacaran Donushantuo Formation, Yangtze Gorges, South China. *Bull. Geosci.* **87**, 183–194 (2012).

Acknowledgments: We thank A. G. Liu, P. C. J. Donoghue, A. R. Prave, T. He, and B. J. W. Mills for contributing to the preparation and valuable discussions and S. N. Rudnev and N. I. Bobkov for assistance in fieldwork and mineral separation. We thank the editor and two anonymous reviewers for their constructive comments. **Funding:** This work was supported by the Strategic Priority Research Program (B) of the Chinese Academy of Sciences (XDB18030300 to M.Z. and X.-H.L. and 26000000 to M.Z.), the National Natural Science Foundation of China (41802029 to C.Y. and 41921002 to M.Z.), the NERC-NSFC program "Biosphere Evolution, Transitions, and Resilience" (NEE6066N/01 to D.J.C.), United States National Science Foundation Frontier Research in Earth Sciences Grant (EAR-2021319 to A.D.R.), and Russian Science Foundation Grant (20-67-46028 to D.V.G.). **Author contributions:** M.Z., D.J.C., F.A.M., A.D.R., and C.Y. conceived the project. C.Y., M.Z., X.-H.L., A.D.R., F.A.M., C.H., and D.V.G. conducted field work and sampling. C.Y. and A.D.R. processed the samples for radio-isotopic analyses. C.H. conducted the carbonate carbon and oxygen isotope measurement. F.T.B. compiled the Ediacaran-Cambrian carbonate carbon isotopic data. C.Y. wrote the first draft of the manuscript, with all authors contributing to the final document. **Competing interests:** The authors declare that they have no competing interests. **Data and materials availability:** All data needed to evaluate the conclusions in the paper are present in the paper and/or the Supplementary Materials.

Submitted 16 April 2021
Accepted 15 September 2021
Published 3 November 2021
10.1126/sciadv.abi9643